

Animal Model

Pathologic Characterization of Short-Chain Acyl-CoA Dehydrogenase Deficiency in BALB/cByJ Mice

Dawna L. Armstrong, Michael L. Masiowski, and Philip A. Wood

Department of Pathology, Baylor College of Medicine, Houston, Texas (D.L.A., M.L.M.); and Department of Comparative Medicine, Schools of Medicine and Dentistry, University of Alabama, Birmingham, Alabama (P.A.W.)

BALB/cByJ mice have a deficiency of short-chain acyl-CoA dehydrogenase (SCAD) and are a useful model for studying the inborn errors of fatty acid metabolism which affect humans. Patients with some of these disorders present with hypoglycemia, hyperammonemia, and microvesicular fatty change of hepatocytes. In the present study we examined pathogen-free, SCAD deficient BALB/cByJ mice and control BALB/cBy mice for biochemical and tissue changes following fasting or salicylate challenge. We observed mitochondrial swelling and microvesicular fatty changes in hepatocytes in mutant mice, especially severe following a fast. However, fasting did not alter their blood ammonia and there was no apparent clinical disease. Similarly, salicylates did not produce disease in the BALB/cByJ mice. We did detect in mice an alternative pathway for salicylate metabolism, by-passing glycine conjugation which is the principal metabolic pathway in humans.

© 1993 Wiley-Liss, Inc.

KEY WORDS: short-chain acyl-CoA dehydrogenase, BALB/cByJ, Reye-like syndrome, morphology, biochemistry, salicylate metabolism

INTRODUCTION

Several inborn errors of β -oxidation of fatty acids have been described in children. Children with acyl-CoA dehydrogenase deficiency have acute episodes of hypoglycemia, metabolic acidosis, and hyperammonemia with prominent microvesicular fatty change of liver [Greene et al., 1988] associated with fasting. The recog-

nition of these metabolic diseases is confusing due to clinical similarities with Reye syndrome (RS) [Greene et al., 1988]. Classic RS is an acute, potentially fatal metabolic episode characterized by hyperammonemia, hypoglycemia, and fatty change of the liver [Reye et al., 1963], and its pathogenesis is understood poorly, but it appears to be associated with salicylate ingestion by children during acute infectious disease episodes [Hurwitz, 1989]. Recently, we described a mutant mouse line with short-chain acyl-CoA dehydrogenase (SCAD) deficiency [Wood et al., 1989] that appears to be a useful animal model in which to study the clinical, biochemical and morphologic expression of inborn errors of fatty acid oxidation. We have shown previously that these mutant mice develop a marked microvesicular fatty change in liver as compared to controls following an 18 hour fast [Wood et al., 1989].

In this report we describe the histopathologic and ultrastructural morphology, and some of the biochemical characteristics found in specific pathogen free (SPF) BALB/cByJ mice in 3 experimental paradigms; non-fasted, fasted, and following a salicylate challenge. The non-fasted state represents the non-provocative condition. The fasted state requires metabolic pathways involved in the β -oxidation of fatty acids. The salicylate challenge was studied because salicylates have been implicated in provoking RS in children [Hurwitz, 1989]. In these situations all mice remained clinically normal in spite of biochemical and morphologic abnormalities. Our results are compared with the morphologic and biochemical changes associated with acutely fatal disease in children with RS and in BALB/cByJ mice [Brownstein et al., 1984] infected by mouse coronavirus or rotavirus.

MATERIALS AND METHODS

BALB/cByJ mice (J mutant mice) and the predecessor control strain, BALB/cBy (Y control mice), were obtained from the Jackson Laboratory (Bar Harbor, Maine) and subsequently propagated at the Baylor College of Medicine and the University of Alabama at Birmingham. All mice were documented to be free of the common rodent pathogenic viruses, including mouse coronavirus and rotavirus, by routine health surveillance including serologic testing by Microbiological Associates or Charles River Laboratories. All mice were

Received for publication May 17, 1993; revision received June 4, 1993.

Address reprint requests to Philip A. Wood, Department of Comparative Medicine, University of Alabama, Birmingham, AL 35294-0019.

maintained specific pathogen free using the microisolator system (Lab Products).

Mice of each strain and both sexes, 6–8 weeks old, were killed humanely by inducing anesthesia with avertin (2,2,2-tribromoethanol) and immediate exsanguination by cardiac puncture following an 18 hour food fast or without fasting. Necropsies were performed immediately and portions of liver, brain, kidney, heart, and skeletal muscle were either fixed in 3% glutaraldehyde for ultrastructural examination, 10% buffered formalin for histologic examination, or frozen in liquid nitrogen for histochemical studies. The tissues were stained with hematoxylin and eosin for documentation of tissue morphology, Oil Red O (ORO) for demonstration of neutral lipid, modified Gomori trichrome for demonstration of mitochondria, and NADH for demonstration of oxidative enzyme activity in mitochondria and cytosol. This marker, rather than succinic dehydrogenase or cytochrome C oxidase, was used for mitochondria because in our experience it provides a more reliable obvious marker for increased mitochondrial number or size [Dubowitz and Brooke, 1973]. All morphologic evaluations were done by subjective examination.

Blood collected for ammonia studies was obtained by cardiac puncture using sodium heparin anticoagulant. Blood was chilled immediately on ice, briefly, then centrifuged to remove the plasma. Plasma ammonia was

measured using a glutamate dehydrogenase assay (Sigma Chemical Co.). Plasma glucose was determined using a glucose oxidase method (Sigma Chemical Co.). Urea cycle enzymes were assayed on liver homogenates as described previously [Nuzum and Snodgrass, 1976].

Groups of Y control mice and J mutant mice (all 7–8 weeks old) were dosed daily for 3 consecutive days with 150 mg/kg sodium salicylate intraperitoneal (IP) followed by an 18 hour fast. Urinary organic acids were evaluated as described previously using gas chromatography-mass spectrometry [Wood et al., 1988].

All mouse experiments were done in accordance with procedures approved by the animal use committees of both Baylor College of Medicine and the University of Alabama at Birmingham.

Statistical Analyses

All results were analyzed for statistically significant differences using either a one way analysis of variance or Student's t-test using the Statistix program (Analytical Software). The level of significance was set at $P < 0.05$. The numbers of mice used in each experimental group are given in the data tables.

RESULTS

All animals appeared clinically normal at the time of sacrifice, and the organs had no gross lesions, except for

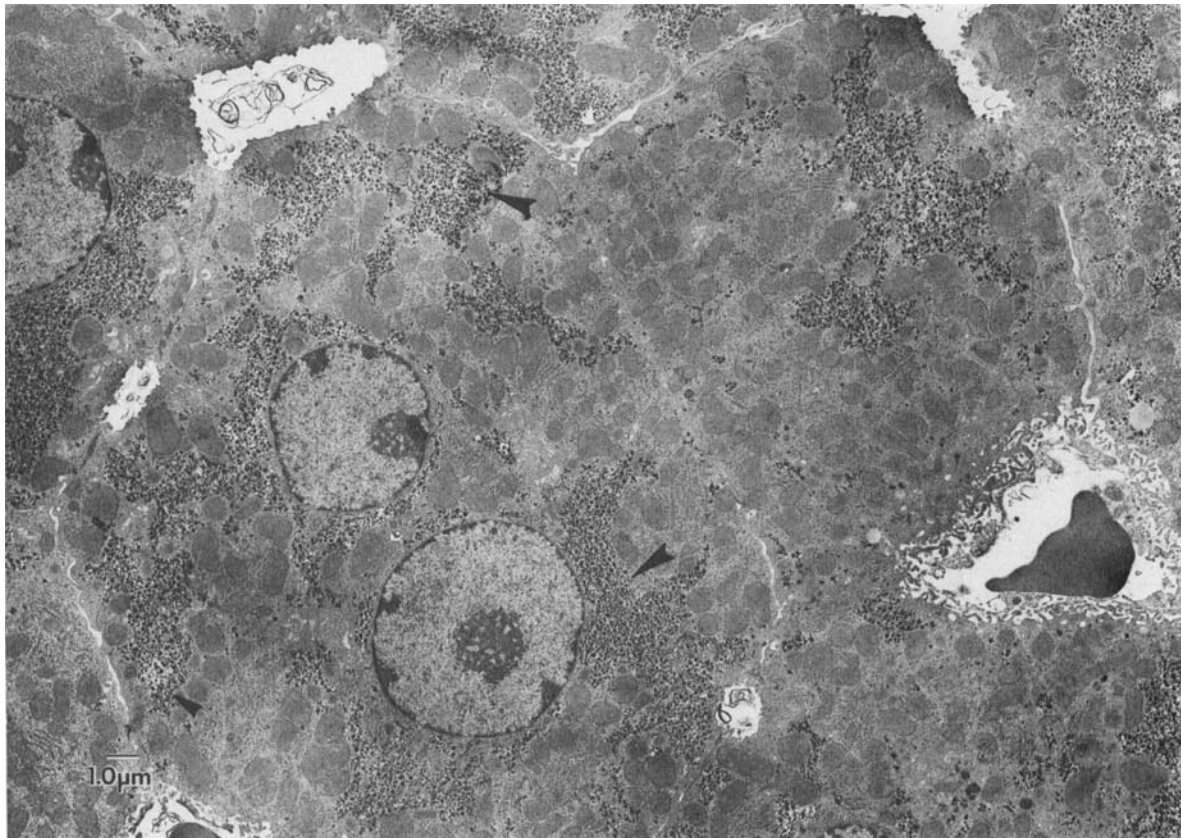


Fig. 1. BALB/cBy mouse liver, nonfasted showing prominent glycogen (solid arrows), regular dense mitochondria and no lipid ($\times 4,600$). Bar indicates 1 μm .

the livers of fasted BALB/cByJ mice, which were smooth, pale, and felt greasy.

Morphologic Observations

Liver. The livers of nonfasted Y control mice contained minute amounts of Oil Red O positive staining lipid, which was confirmed by electron microscopy. Oxidative enzyme stains disclosed a diffuse dense reaction for NADH. Modified Gomori stain identified no abnormal mitochondria and electron microscopy (EM) showed normal mitochondria with regular round to oval shapes, a dense matrix and well defined cristae. The glycogen content was prominent (Fig. 1).

Livers of fasted Y control mice had increased lipid with vesicles ranging from 1 to 3 μm in diameter, which was confirmed by EM. Mitochondria had more prominent staining with NADH and modified trichrome, and by EM were larger, and more irregular than those of normal, nonfasted mice. The matrix density was not changed. There was less glycogen (Fig. 2) than in nonfasted animals (Fig. 1).

Livers of the nonfasted J mutant mice had increased neutral fat. Hepatocytes contained vesicles of neutral lipid which ranged in size from 1 to 3 μm . Electron microscopy demonstrated variation in the shape of the mitochondria, decreased glycogen, increased lipid drop-

lets with mitochondria wrapping around some of the lipid droplets (Figs. 3, 4).

Livers of fasted J mutant mice had marked increase in lipid, with droplets ranging from 1 to 8 μm . The entire section stained with ORO fat stain was red at low power, and almost every cell was involved with this accumulation of lipid, which was indistinguishable from liver lesions demonstrated previously [Wood et al., 1989]. Mitochondrial stains showed increased intensity of staining compared with the nonfasting animals. This was confirmed by EM in which mitochondria had increased size and irregular shape, decreased matrix granules and almost no glycogen (Figs. 5, 6).

Other organs. Kidneys of nonfasted Y controls had some small (1 μm) lipid droplets in the collecting tubules, especially in the proximal tubules. Fasted Y controls had more lipid with droplets ranging up to 3 μm in diameter. Kidneys of nonfasted J mutants had some lipid in focal zones of the proximal tubules and contained similar amounts of lipid in collecting tubules. There was no demonstration of neutral lipid in skeletal muscle by Oil Red O staining in mice of any group. There was equivocal increased staining of mitochondria in the skeletal muscle of J mutants compared with control animals both, before and after fasting. Light microscopy of the heart in control and mutant mice showed no changes. Light microscopy of the brains of the control

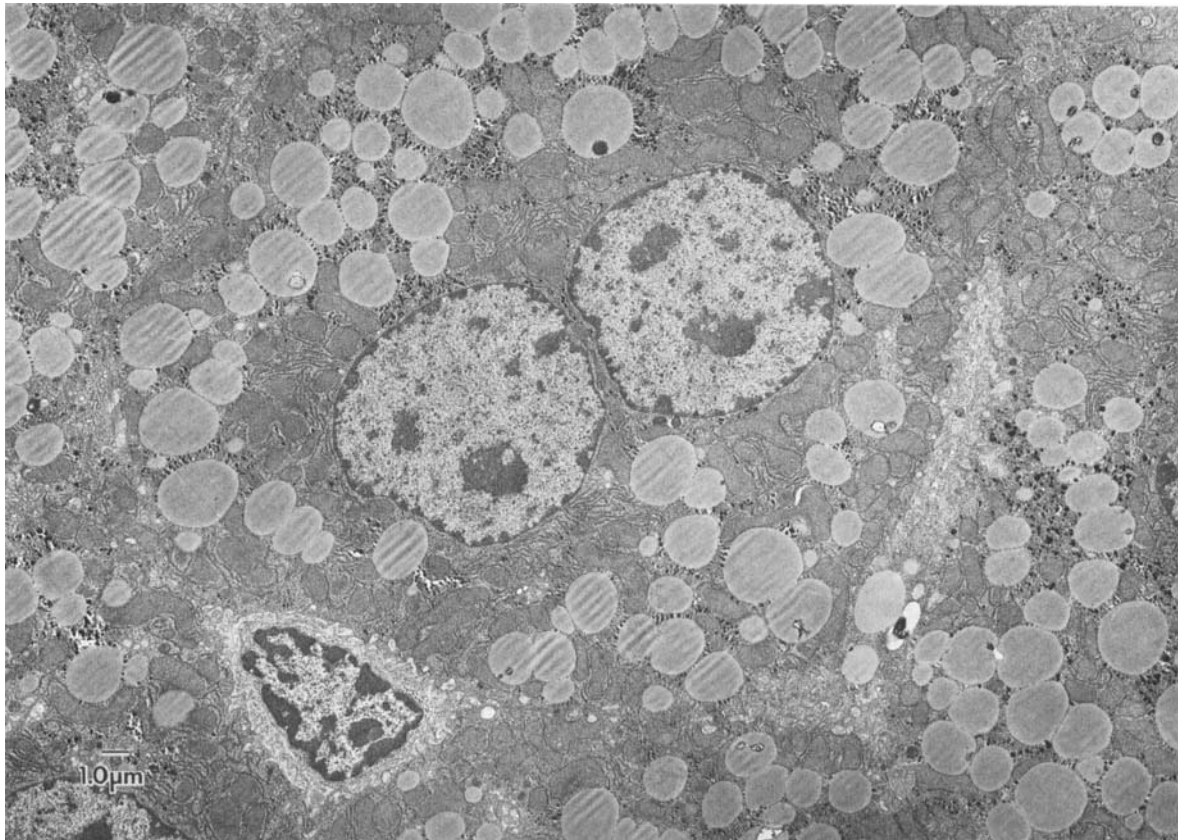


Fig. 2. BALB/cBy mouse liver, fasting showing less glycogen than control in Figure 1 ($\times 4,600$). Bar indicates 1 μm .

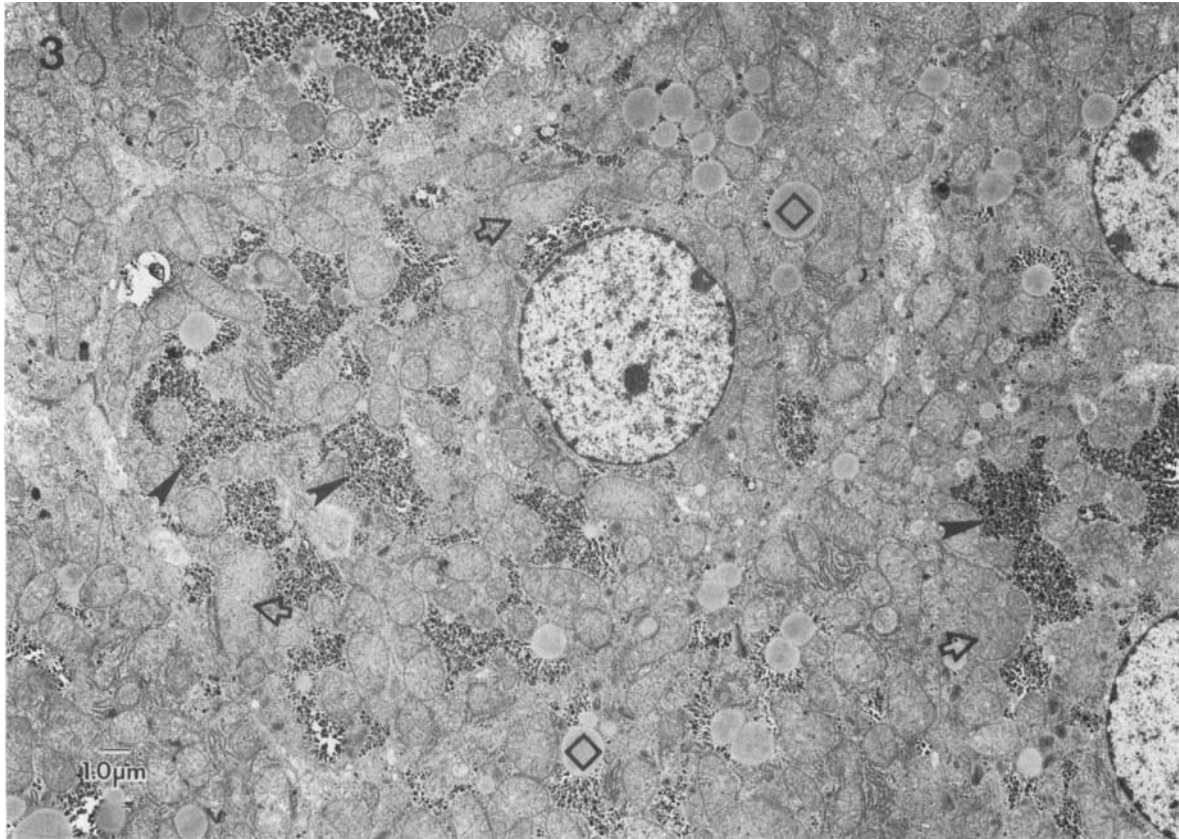


Fig. 3. BALB/cByJ mutant mouse liver, nonfasted showing prominent glycogen (open arrows), irregular mitochondria, and prominent neutral lipid (open diamonds) ($\times 4,600$). Bar indicates 1 μm .

and mutant mice in the nonfasting and fasting state showed no lesions. Results of morphologic studies in J mutant mice, and Y control mice are summarized in Table I.

Biochemical Analyses

Ammonia concentration was determined in plasma of J and Y mice (4–12 weeks old) in either the nonfasting state or following an 18 hour fast. Results compiled in Table II demonstrate that specific pathogen-free, nonfasted or fasted J mutant mice have only a slight elevation in plasma ammonia compared to Y controls. Although fasting ammonia values appeared to be slightly elevated compared to nonfasting values in both strains, none was significantly different from any other. The liver urea cycle enzymes, carbamyl phosphate synthetase and ornithine transcarbamylase, located normally in mitochondria, had the same activities in both genotypes (Table III). Considering that there was no difference in plasma ammonia values, this was the expected result, in spite of very abnormal mitochondrial morphology.

Salicylate challenge failed to produce any clinical signs in any mice. The Y mice readily produced salicylglycine, 5-hydroxysalicylate, and also excreted some free salicylate as determined by gas chromatography–mass spectrometry analysis of urinary or-

ganic acids. The J mutants continued to glycine conjugate butyryl-CoA, producing the usual large amounts of butyrylglycine, large amounts of 5-hydroxysalicylate and some free salicylate with only traces of salicylglycine. The relative abundance ratios of these metabolites are shown in Table IV.

Relative amounts of each metabolite were calculated by determining the ratio of the specific metabolite abundance divided by the internal standard abundance. Internal standard (malonic acid) was added based on the creatinine concentration of the urine sample [Wood et al., 1988]. As shown in Table IV, there was no reduction in the ability of the mutant J mice to conjugate butyryl-CoA in spite of the added metabolite salicylate, compared to untreated J mutants. There appears to be reduction, although not statistically significant, in production of 5-hydroxylated salicylate in J mutants, as compared to Y controls.

DISCUSSION

Children with defects in β -oxidation of fatty acids, particularly medium chain acyl-CoA dehydrogenase (MCAD) deficiency, have been described with illness partially mimicking RS [Bougneres et al., 1985; Roe et al., 1986]. There is a wide range of clinical presentations of β -oxidative defects and the biochemical alterations are complex. In the most severe form, acute episodes

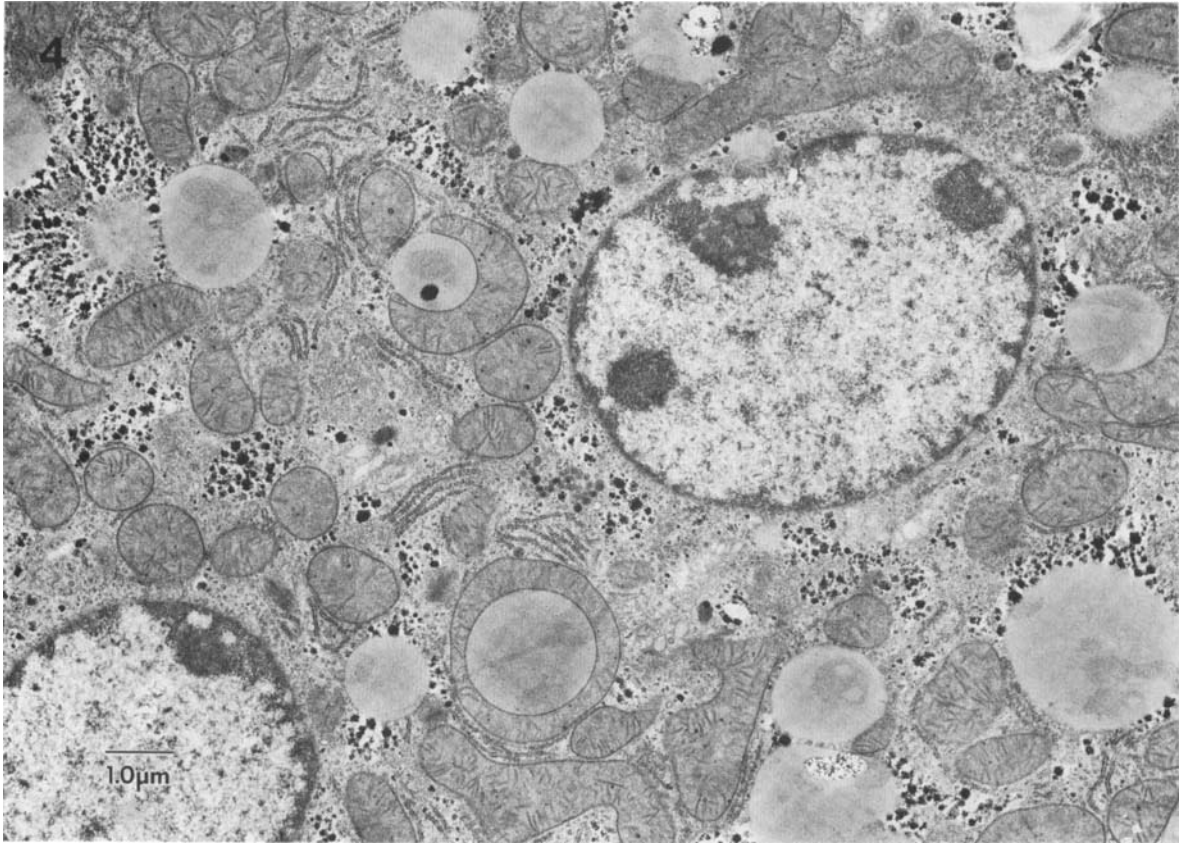


Fig. 4. BALB/cByJ mutant mouse liver, nonfasted showing bizarre shaped mitochondria with dense granules ($\times 23,000$). Bar indicates 1 μm .

include metabolic acidosis, nonketotic hypoglycemia, hyperammonemia, and dicarboxylic aciduria, depending on the specific acyl-CoA dehydrogenase deficiency. These children may die or recover from such life-threatening episodes. The pathogenesis of this episodic presentation is not understood fully. Demonstrated by Brownstein et al. [1984], spontaneous viral infections in the BALB/cByJ mice, now known to be SCAD deficient, provides a possible etiological event for the precipitation of a RS-like illness in combination with an inherited metabolic defect. This parallels the experience in children with one of several inborn errors, including β -oxidation defects and infection resulting in a RS-like illness Greene et al. [1988].

There are similarities of morphologic changes in the fasted J mice as summarized in Table I and human RS. Mouse lesions appear similar to grade 2 (moderate) RS in human patients as described by Daugherty et al. [1987]. Human RS has been associated with characteristic histopathological alterations. Grossly, cerebral edema and fatty liver have been the hallmarks of the disease process if examined at a time when symptoms peak. The liver has received the most attention and has microvesicular fat accumulation or foaminess without necrosis or inflammation.

Lipid droplets, as well as changes in the mitochondria (Fig. 7) as visualized by electron microscopy have been

considered to be most useful in making the diagnosis of human RS. There is increased size of mitochondria [Partin et al., 1971; Schubert et al., 1972; Daugherty et al., 1987] which correlates with the clinical severity of the disease. There are decreased numbers of matrix dense granules [Partin et al., 1971; Schubert et al., 1972; Iancu et al., 1977; Daugherty et al., 1987]. The shape of the mitochondria becomes irregular, pleomorphic, and often amoeboid [Daugherty et al., 1987]. The smooth endoplasmic reticulum proliferates, the peroxisomes increase in numbers and glycogen decreases, according to the severity of the disease. The matrix density tends to decrease.

Liver histopathology of human RS and human MCAD deficiency are similar at light microscopy, with microvesicular steatosis very prominent. Ultrastructural characteristics of MCAD deficient liver mitochondria are quite variable. The mitochondrial matrix swelling and rarefaction characteristic of RS are not seen in human MCAD deficiency. In a study of 7 MCAD deficient patients [Treem et al., 1986], mitochondria from three liver biopsies showed increased matrix density. One biopsy disclosed intramitochondrial crystalloid structures, and three biopsies showed normal mitochondria [Treem et al., 1986].

The human brain in RS [Partin et al., 1975, 1978] has watery swelling of the astrocytes and pyknosis of some

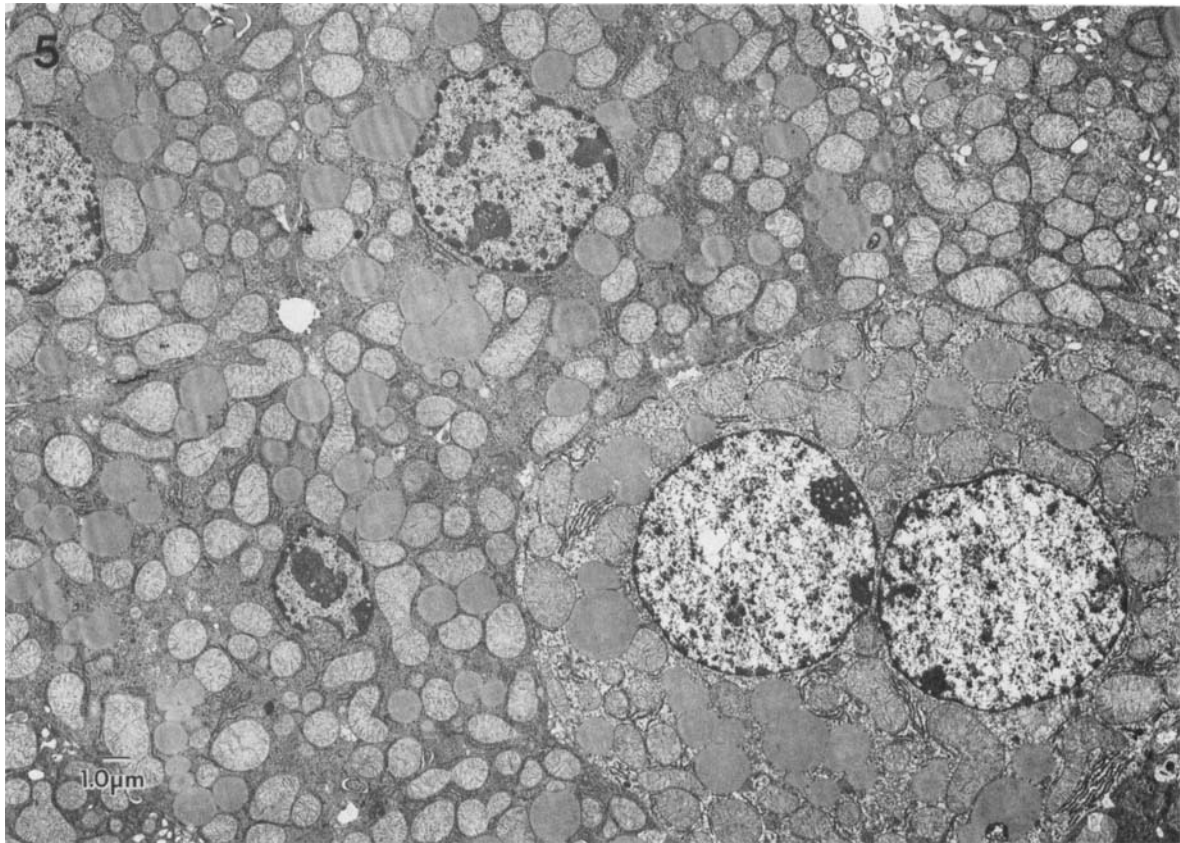


Fig. 5. BALB/cByJ mutant mouse liver, fasting showing increased lipid, very irregular swollen mitochondria with decreased matrix density ($\times 4,600$). Glycogen content is less than nonfasted control and mutant mice. Bar indicates 1 μ m.

TABLE I. Subjective Comparison of Morphologic Features of SCAD Deficiency in BALB/cByJ Mice*

Morphology	Nonfasting		Fasting	
	Y controls	J mutants	Y controls	J mutants
Liver				
Lipid	+	++	++	++++
Mitochondria				
Size	++	++	++/+++	++++
Shape	Normal	Irregular	Normal	Swollen
Matrix	++++DG	++/+++	++/+++	+
Peroxisomes	ND	ND	ND	ND
Glycogen	++++	++	++	±
Brain				
Lipid	NP	NP	NP	NP
Mitochondria No.	+	+	+	+
Size	+	+	+	+
Shape	+	+	+	+
Astrocytes	+	+	+	+
Kidney				
Lipid	+	+	++	++
Heart				
Lipid	+	+	+	+
Mitochondria	NE	NE	NE	NE
Muscle				
Lipid	+	+	+	+
Mitochondria	+	++	+	++

* Glossary: + = quantitation of the amounts of glycogen and lipid, and mitochondrial size and matrix density was evaluated by comparison with the control amounts in the nonfasted Y control mice. DG = dense granules; NE = not examined; ND = not determined; NP = not present. The various organs were examined from two mice of each genotype and fed state.

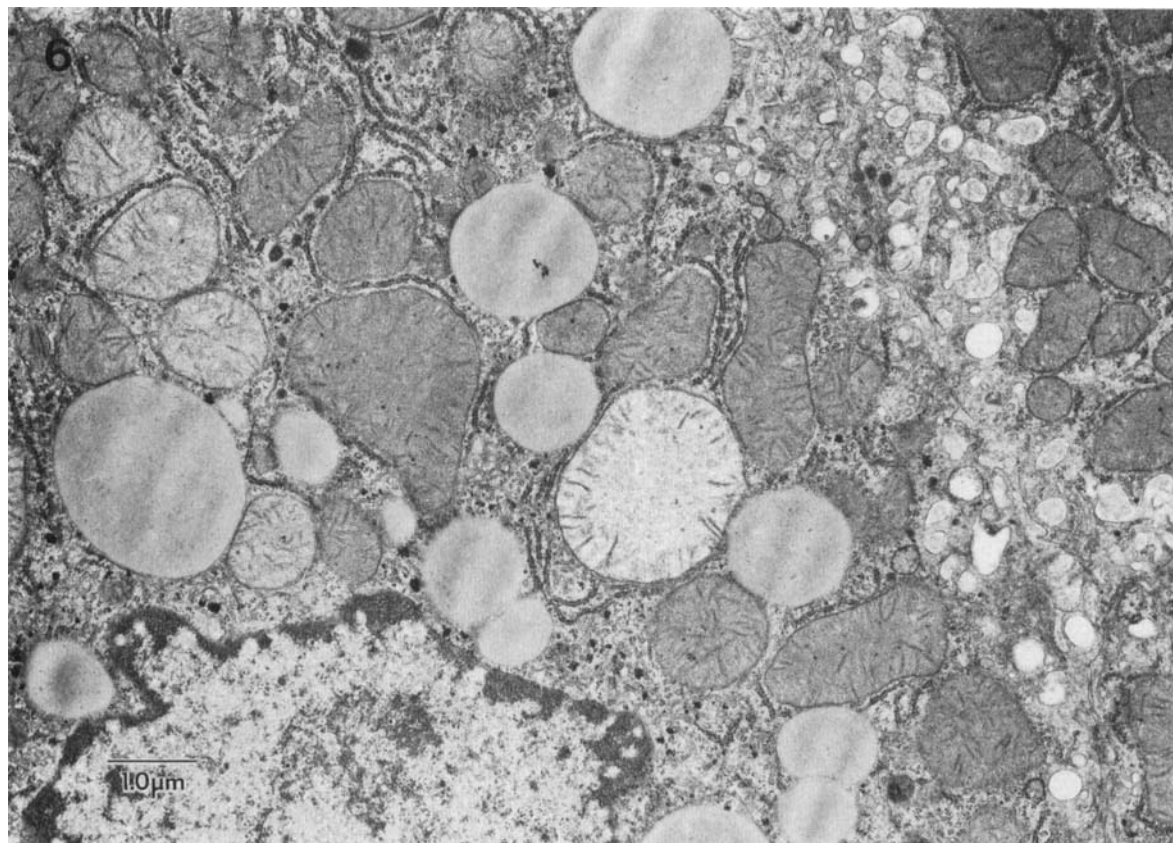


Fig. 6. BALB/cByJ mutant mouse liver, fasting demonstrating prominent lipid, decreased glycogen and irregular swollen mitochondria with decreased matrix density ($\times 15,180$). Bar indicates 1 μm .

of the nuclei of neurons, but no inflammation. Neutral lipid stains of the brain demonstrate no accumulation of neutral lipid. By electron microscopy there are osmophilic deposits in pericytes [Chang et al., 1973]. There is astrocyte swelling and deglycogenation. There are blebs in the myelin and there is injury of the mitochondria of the neuronal cell bodies, but not the processes. Mitochondria have a pleomorphic appearance with irregular outer membranes, and these cristae appear normal, but the matrix is expanded. Although the fasted J mutant mice show most of the morphologic changes seen in the liver of patients with RS, brain lesions are not present in clinically normal J mice, however brain lesions in J mutant mice, similar to those found in human RS, were described by Brownstein et al. [1984].

We performed a salicylate challenge of control and mutant mice to examine a possible competitive inhibition of butyrylglycine formation by salicylate glycine

conjugation. The goal in this experiment was to model the hypothetical situation of a child with MCAD deficiency, who is presumably dependent on glycine conjugation of suberyl-CoA and hexanoyl-CoA for maintaining an asymptomatic state. Theoretically such a child challenged by an infectious disease or another stressful situation might be challenged additionally with aspirin which would require glycine to form salicylglycine [Goodman et al., 1980]. In man, approximately 75% of urinary salicylate metabolites is in the form of salicylglycine [Goodman et al., 1980]. A possible outcome for such glycine competition would be acute clinical disease, thus providing an explanation for the incrimination of aspirin in the etiology of RS-like illness in an MCAD deficient child dependent on glycine conjugation as an alternative pathway for normal metabolic function. However, we were unable, in our model, to interfere with the butyryl-CoA/glycine conjugation with salicy-

TABLE II. Plasma Ammonia Concentration ($\mu\text{mol/L}$)*

Genotype (age)	Nonfasting	Genotype (age)	Fasting
Y controls n=5 (6–12 wk)	120(49)	Y controls n=9 (6–8 wk)	164(40)
J mutants n=6 (4–6 wk)	157(50)	J mutants n=9 (4–10 wk)	198(63)

* Values given are \bar{x} (S.D.).

TABLE III. Mitochondrial Urea Cycle Enzyme Activity (nmol/min/mg Liver Protein)*

Genotype	Carbamylphosphate synthetase	Ornithine transcarbamylase
Y controls n=4	1.07 (0.283)	103 (10.0)
J mutants n=4	1.13 (0.158)	100 (15.7)

*Values are \bar{x} (S.D.). 18 hour fast—6 weeks old.

TABLE IV. Urinary Metabolites—Salicylate Challenge Experiment—Relative Abundance Ratio*

Mice and treatment	Malonate (IS)	Salicylate	5-Hydroxysalicylate	N-butyrylglycine
Salicylate challenged J mutant mice n=5	1	0.76 (0.76)	0.45 (0.38)	7.6 (7.0)
Salicylate challenged Y controls n=6	1	0.99 (1.0)	2.3 (1.9)	0
Nonsalicylate challenged J mutant n=3	1	0	0	8.0 (4.7)

*All mice were 6–8 weeks old and all urines were collected after the 18 hour fast as described in Methods. Values given are the \bar{x} (S.D.). Internal standard (IS) was added to the urine based on the creatinine concentration [Wood et al., 1988] to normalize metabolite values. Using Student's t-test, there were no significant differences between ratios for salicylate and 5-hydroxysalicylate in controls and mutants having the salicylate challenged, as well as no significant differences in the ratios for butyrylglycine excretion between salicylate or nonsalicylate challenged mutants. We were unable to quantify the salicylglycine due to co-elution with stearic acid. We could qualitatively evaluate these two compounds based on their distinct mass spectra.

late. The dose chosen was 2–3 times higher than the usual human dose of aspirin. It is unknown what happens to glycine conjugation of suberyl and hexanoyl-CoAs, in human MCAD deficiency treated with salicylates. Our experiment demonstrated that mice 5-hydroxylate salicylate very efficiently compared to the normal human, in whose urine, this metabolite only accounts for <1% of total salicylate metabolites [Goodman et al., 1980].

Comparisons of the biochemical and pathological changes found in our studies of pathogen-free J mice

with those described by Brownstein et al. [1984] in their mice with the associated corona or rota virus infections, reveal the following. The normal blood ammonia concentrations found in our study is in striking contrast to the severe hyperammonemia ($1,489 \pm 106 \mu\text{mol/L}$) reported in the J mice [Brownstein et al., 1984] infected with mouse coronavirus or rotavirus. We speculate that the hyperammonemia is likely the key metabolic abnormality that causes the potentially fatal clinical signs and lesions of the central nervous system as reported [Brownstein et al., 1984] in infected J mice. Therefore

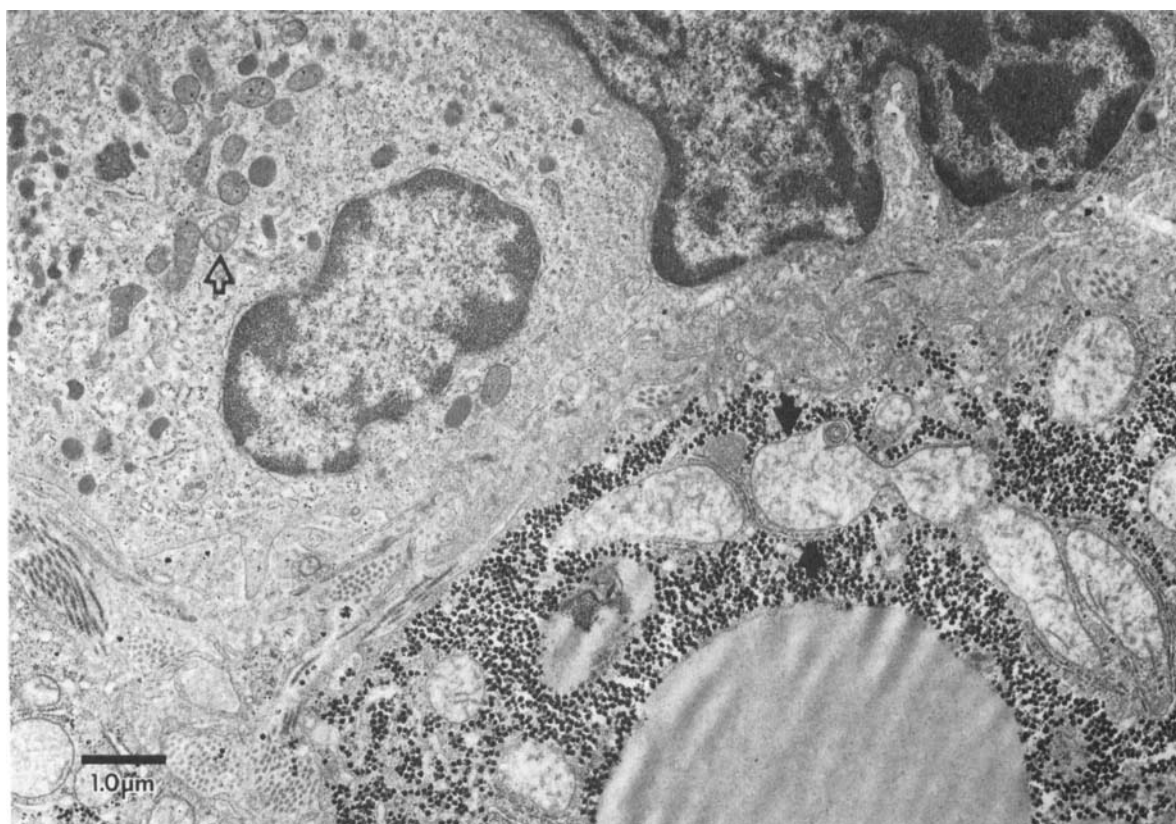


Fig. 7. Liver in human RS, electron micrographs showing lipid (open diamond) in hepatocyte with large mitochondria (solid arrow), with decreased matrix granules and pleomorphic shape. The mitochondria in adjacent Kupffer cell (open arrow) serves as an internal control. Bar indicates 1 μm .

viral infection possibly plays a critical role in the pathogenesis of an acute, fatal disease episode in J mutant mice, possibly by inducing a hyperammonemia. Pathogen-free J mice fasted in our study developed hypoglycemia [Wood et al., 1989] and hepatic steatosis with ultrastructural mitochondrial changes, but remained clinically normal. We speculate that SCAD deficiency, found specifically in these mice, is the other critical factor in the pathogenesis of the syndrome, because Brownstein et al. [1984] observed that other mouse strains were infected, but did not develop the syndrome. We believe that this is an exciting model to pursue for studying the possible combined pathogenetic factors of genetics and infectious disease in the production of a serious, potentially fatal disease of children.

ACKNOWLEDGMENTS

This work was supported by NIH grant RO1-RR02599 (P.A.W.). We thank Mr. Doug Hamm for his expert technical assistance and Mr. Jim Barrish for preparing the electron micrographs.

REFERENCES

- Bougneres PF, Rocchiccioli F, Kolvaa S, Hadchouel M, Lalau-Keraly J, Chaussain J-L, Wadman SK, Gregersen N (1985): Medium-chain acyl-CoA dehydrogenase deficiency in two siblings with a Reye-like syndrome. *J Pediatr* 106:918-921.
- Brownstein DG, Johnson EA, Smith AL (1984): Spontaneous Reye's-like syndrome in BALB/cByJ mice. *Lab Invest* 51:386-395.
- Chang LW, Gilbert EF, Tanner W, Moffat HL (1973): Reye syndrome: Light and electron microscopic studies. *Arch Pathol Lab Med* 96:127-132.
- Daugherty CC, Gartside PS, Heubi JE, Saalfeld K, Snyder J (1987): A morphometric study of Reye's syndrome: Correlation of reduced mitochondrial numbers and increased mitochondrial size with clinical manifestations. *Am J Pathol* 129:313-326.
- Dubowitz V, Brooke MH (1973): Histological and histochemical stains and reactions. In Walter JW (ed): "Muscle Biopsy: A Modern Approach, Volume 2. Major Problems in Neurology." Philadelphia: W. B. Saunders Co., pp 19-40.
- Goodman AGG, Goodman LS, Gilman A (1980): "The Pharmacological Basis of Therapeutics." New York: Macmillan, pp 694-695.
- Greene CL, Blitzer MG, Shapira E (1988): Inborn errors of metabolism and Reye syndrome: differential diagnosis. *J Pediatr* 113:156-159.
- Hurwitz ES (1989): Reye's syndrome. *Epidemiol Rev* 11:249-253.
- Iancu TC, Mason WH, Neustein HB (1977): Ultrastructural abnormalities of liver cells in Reye's syndrome. *Hum Pathol* 8:421-431.
- Nuzum CT, Snodgrass PJ (1976): Multiple assays of the 5 urea cycle enzymes in human liver homogenates. In Grisoli S, Bagnena R, Mayor F (eds): "The Urea Cycle." New York: John Wiley and Sons, pp. 325-349.
- Partin JC, Schubert WK, Partin JS (1971): Mitochondrial ultrastructure in Reye's syndrome (encephalopathy and fatty degeneration of the viscera). *N Engl J Med* 285:1339-1343.
- Partin JC, Partin JS, Schubert WK, McLaurin RL (1975): Brain ultrastructure in Reye's syndrome (encephalopathy and fatty alteration of the viscera). *J Neuropathol Exp Neurol* 34:425-444.
- Partin JS, McAdams AJ, Partin JC, Schubert WK, McLaurin RL (1978): Brain ultrastructure in Reye's disease. II. Acute injury and recovery processes in three children. *J Neuropathol Exp Neurol* 37:796-819.
- Reye RDK, Morgan G, Baral J (1963): Encephalopathy and fatty degeneration of the viscera: a disease entity in childhood. *Lancet* 2:749-752.
- Roe CR, Millington DS, Maltby DA, Kinnebrew P (1986): Recognition of medium-chain acyl-CoA dehydrogenase deficiency in asymptomatic siblings of children dying of sudden infant death or Reye-like syndromes. *J Pediatr* 108:13-18.
- Schubert WK, Partin JC, Partin JS (1972): Encephalopathy and fatty liver (Reye's syndrome). In Popper H, Schaffner F (eds): "Progress in Liver Disease." New York: Grune and Stratton, pp. 489-510.
- Treem WR, Witzleben CA, Piccoli DA, Stanley CA, Hale DE, Coates PM, Watkins JB (1986): Medium-chain and long-chain acyl-CoA dehydrogenase deficiency: clinical, pathologic and ultrastructural differentiation from Reye's syndrome. *Hepatology* 5:1270-1278.
- Wood PA, Armstrong D, Sauls D, Davisson MT (1988): Screening mutant mice for inborn errors of metabolism. *Lab Anim Sci* 38:15-19.
- Wood PA, Amendt BA, Rhead WJ, Millington DS, Inone F, Armstrong D (1989): Short-chain acylcoenzyme: a dehydrogenase deficiency in mice. *Pediatr Res* 25:38-43.